

## Spectrophotometric analysis of stability of gold nanoparticles during catalytic reduction of 4-nitrophenol

Farhat SAIRA<sup>1</sup> , Samia SALEEMI<sup>2</sup> , Humaira RAZZAQ<sup>3</sup> , Rumana QURESHI<sup>2\*</sup> 

<sup>1</sup>Nanoscience and Technical Division, National Centre for Physics (NCP), Islamabad, Pakistan

<sup>2</sup>Department of Chemistry, Quaid-i-Azam University, Islamabad, Pakistan

<sup>3</sup>Department of Chemistry, University of Wah, Rawalpindi, Pakistan

Received: 19.04.2020 • Accepted/Published Online: 13.10.2020 • Final Version: 17.02.2021

**Abstract:** Spectrophotometric monitoring of 4-nitrophenol (4-NP) reduction by sodium borohydride ( $\text{NaBH}_4$ ) using gold nanoparticles (GNPs) as a catalyst has been extensively studied, but the stability of GNPs in terms of change in the surface plasmon resonance (SPR) at different temperatures has not been explored. In the present investigation, our aim was to evaluate the SPR stability of GNPs as a catalyst during the reduction of 4-NP at different elevated temperatures (i.e. 30–60 °C) and sodium borohydride concentrations. Sensitivity of this degradation process toward concentration of GNPs at a range of temperatures is also evaluated. The spectrophotometric results reveal that up to 45 °C, 12 ± 1.5 nm catalyst has a consistent optical density (OD) during the entire 4-NP reduction process, which is related to the surface integrity of catalyst atoms. As the temperature approached 50 °C, the OD gradually decreased and showed a blue shift as the reaction proceeded, which could be related to a decrease in particle size or surface dissolution of gold atoms. The present study may find application in the design of catalysts for the reduction of organic pollutants in industrial wastewater at a range of temperatures.

**Key words:** Spectrophotometry, gold nanoparticles, surface plasmon resonance, optical density, rate constant

### 1. Introduction

Pal et al. were the first to identify catalyst-mediated conversion of 4-nitrophenol (4-NP) to 4-aminophenol (4-AP) [1]. The product of this reaction is 4-AP, an effective intermediate in the synthesis of painkillers. There are other uses for it in the photographic and cosmetic industries. Thermodynamics predict the feasibility of this process, but kinetically this reaction is not favorable, i.e. it does not occur in the absence of a catalyst if left for 2 days [2]. This reduction reaction is feasible in the presence of a nanocatalyst. Reaction monitoring is usually carried out by UV-Vis spectroscopy at a 400-nm wavelength. Spectrophotometry is a method applied to assess the quantitative level of an analyte in a particular solution. The basic principle is the absorption of light at a particular wavelength as it passes through the solution. This information is good enough to calculate different kinetic parameters such as entropy of activation, rate constant, activation energies, and frequency factor [3–5]. Organic pollutants are removed by various techniques from industrial wastes, including photocatalysis, membrane filtration, chemical precipitation, physical adsorption, and catalytic degradation. The present degradation method to remove organic pollutant is a simple, efficient, and applicable technique which is an alternative green method, because it has low energy consumption and does not produce a large amount of metal oxide sludge [6].

Gold nanoparticles (GNPs) possess fascinating optical, chemical, and electronic properties; because of these properties, they are used in the fields of catalysis, electronics, and biomedicine. In the field of catalysis, much higher rates than bulk metal have been reported owing to the unique properties of nanocrystals in catalyzing different reaction types [7–14]. Unsaturated valencies of surface atoms render nanocrystals with relatively higher surface energies. Size, shape, concentration, and temperature have been the variables focused on through the years for catalytic testing of nanomaterials [15–39]. However, the stability of the catalyst during the course of a catalytic reaction has not been reported in detail at different ranges of temperatures and concentrations of borohydride (BH). Previously, the SPR stability of gold nanoparticles has been evaluated for the reduction of potassium hexacyanoferrate (III) at room temperature only; it was observed that SPR remained stable over the course of the reduction reaction [20]. This fact is reported in detail in the Discussion section. Conversion of 4-NP and potassium ferricyanide by SBH is used as a model reaction [17–19].

\* Correspondence: r\_quresh@qau.edu.pk

## 2. Materials and methods

All of the required chemicals for the present study were of analytical grade and were used as received. A previously reported method was used to synthesize GNPs (gold nanoparticles) of  $12 \pm 1.5$  nm diameter [40]. Briefly, trisodium citrate (2 mL of 1% solution) was added dropwise to a boiling 20-mL (1 mM) gold salt solution. The solution was stirred until a red color was obtained, and stored in a cold location for further use. A Shimadzu 1601 (Shimadzu, Kyoto, Japan) was used to measure spectroscopic data; TEM at 100 kV (FEI Tecnai Spirit; FEI, Hillsboro, OR, USA) was used to characterize GNPs (Figure 1). Ultrasonication was carried out for 2 min before each catalytic experiment with these GNPs.

The reaction mixture consisted of 100  $\mu$ L each of 8nM GNPs and 1 mM 4-NP added to a standard quartz cuvette. The volume was brought up to 3.5 mL with water. Freshly made and chilled  $\text{NaBH}_4$  (100  $\mu$ L, 100mM) was added to the cuvette. The pale yellow color of the 4-nitrophenol changed immediately to dull green. Spectrophotometric changes were recorded in a time span of 1–3 min according to the reaction conditions. The rate constant was determined depending on experimental factors. An extinction coefficient of  $12 \pm 1.5$  nm NPs was calculated from the UV-Vis spectrum using the method given in the literature [41], and was found to be  $2 \times 10^8 \text{ M}^{-1} \text{ cm}^{-1}$ .

## 3. Results and discussion

GNPs were synthesized using the Frens method [40] and were utilized for catalytic reduction of 4-NP. Spectrophotometric monitoring of stability of GNPs during the course of the reaction was carried out. The stability of GNPs was studied in terms of surface plasmon resonance (SPR), as it is highly sensitive to the chemical environment, i.e. the refractive index of the species surrounding GNPs. SPR is a phenomenon that occurs as a result of the cooperative oscillation of valence electrons in the metallic nanoparticles. This research article deals with this physical phenomenon in GNPs during catalytic reduction reaction.

### 3.1. Stability of GNPs at different temperatures

The stability of GNPs at different temperatures was a new finding for this article. GNPs of  $12 \pm 1.5$  nm diameter were found to be fairly stable at 30, 35, 40, and 45  $^\circ\text{C}$  for the reduction of 4-NP (Figure 2). At the studied range of temperatures, the GNPs were capable of withstanding the constant collisions of reactants and solvent molecules. Additionally, the surface atoms of the GNPs were not dissolved during the course of the reaction, as observed by its consistent OD. However, as the temperature increased from 45 to 50  $^\circ\text{C}$ , signs of catalyst dissolution started to appear, as observed from the gradual decrease in the OD values (Figure 3). This can be inferred from the collisions of reactant as well as solvent molecules against the catalyst surface as a result of their increased kinetic energy at higher temperatures, which leads to the surface atoms' dissolution into the reaction mixture. This process of dissolution continued as the temperature varied from 50 to 60  $^\circ\text{C}$ , but no sign of aggregation was observed (see Figures 2 and 3).

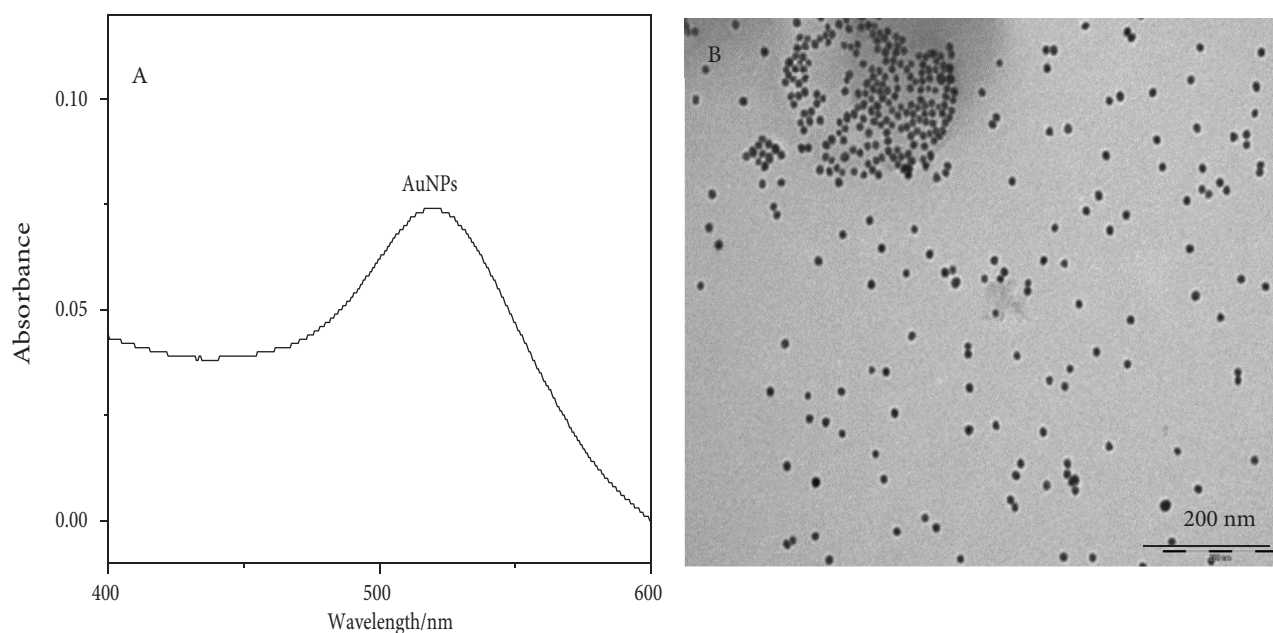


**Figure 1.** UV-visible spectrum (A) and TEM image (B) of gold nanoparticles.

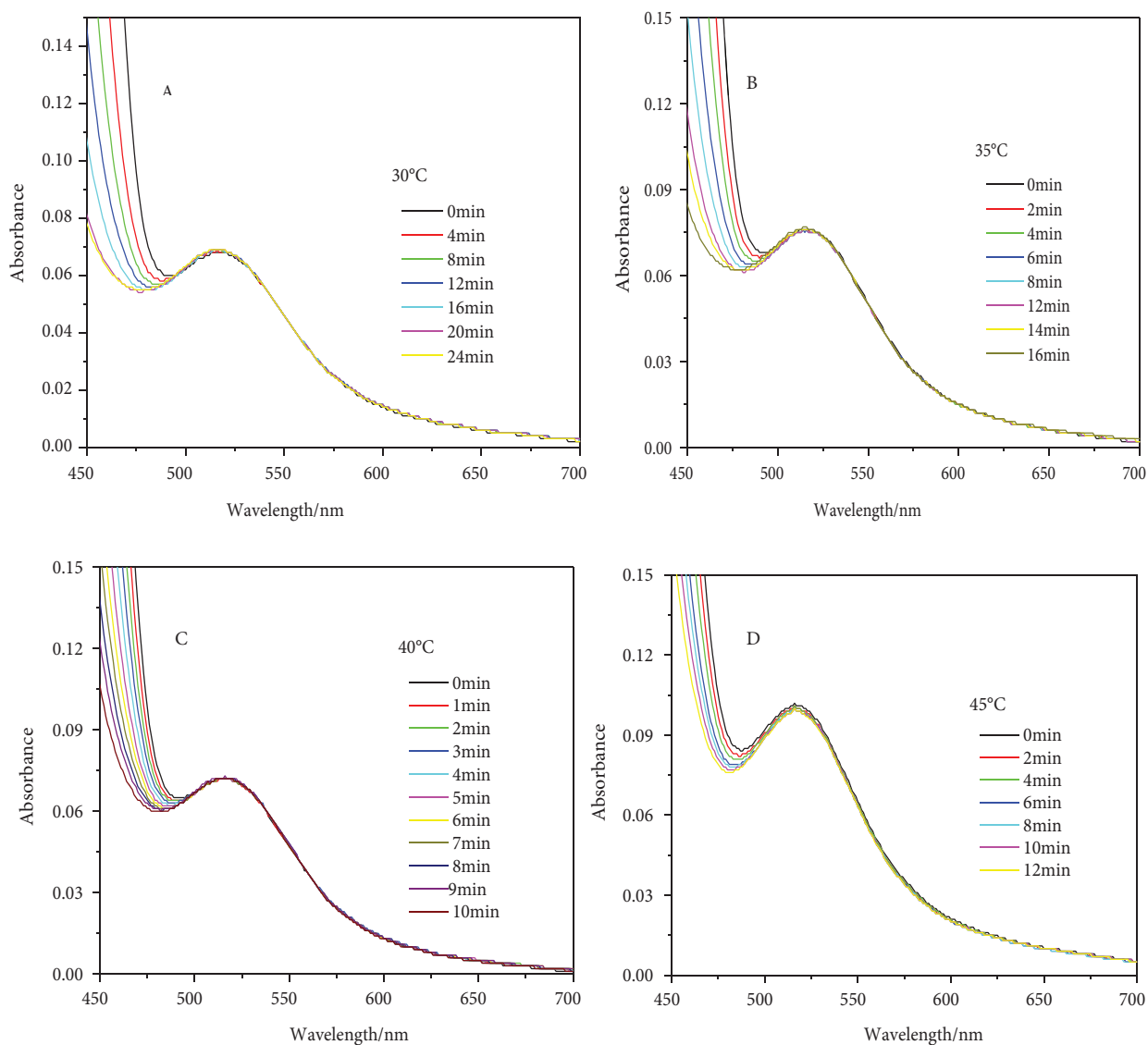


**Figure 2.** Stability of GNPs in terms of their consistent OD at 30 °C (A), 35 °C (B), 40 °C (C), and 45 °C.

Furthermore, the effect of size on the stability of GNPs was examined. For this purpose, 30-nm Au nanoparticles were synthesized and characterized by UV-Vis spectroscopy and TEM as indicated in Figures 4A and 4B. SPR changes for the larger nanoparticles (30 nm) during the reduction of 4-nitrophenol were recorded in the UV-Vis spectra (Figure 4C), and the following conclusion was drawn. The SPR decreased in this case as well, which can be attributed to the dissolution of the surface gold atoms; this is consistent with our previous findings with 12-nm AuNPs. These results for 30-nm AuNPs are different from the results observed for 12-nm AuNPs.

### 3.2. Sensitivity of 4-NP reduction toward GNP concentration

In order to evaluate the sensitivity of this reduction process to GNP concentration, the process was varied from 11.8 nM to 15.5 nM at various temperatures. The kinetic analysis of both of the concentrations was carried out using pseudo-first order kinetics.

$$\ln A = -kt \quad \text{Eq. 1}$$

Plotting  $\ln A$  vs. time, rate constant values were attained [19,20] as shown in Table, where A is depicting absorbance of 4-NP, t is time for reduction, and k is obtained rate constant. It was found that the rate constant of 15.5 nM GNPs was 5.2 times higher than for lower concentrations at 35 °C, 4.9 times higher at 40 °C, and 3.2 times higher at 45 °C as shown in Figure 5.

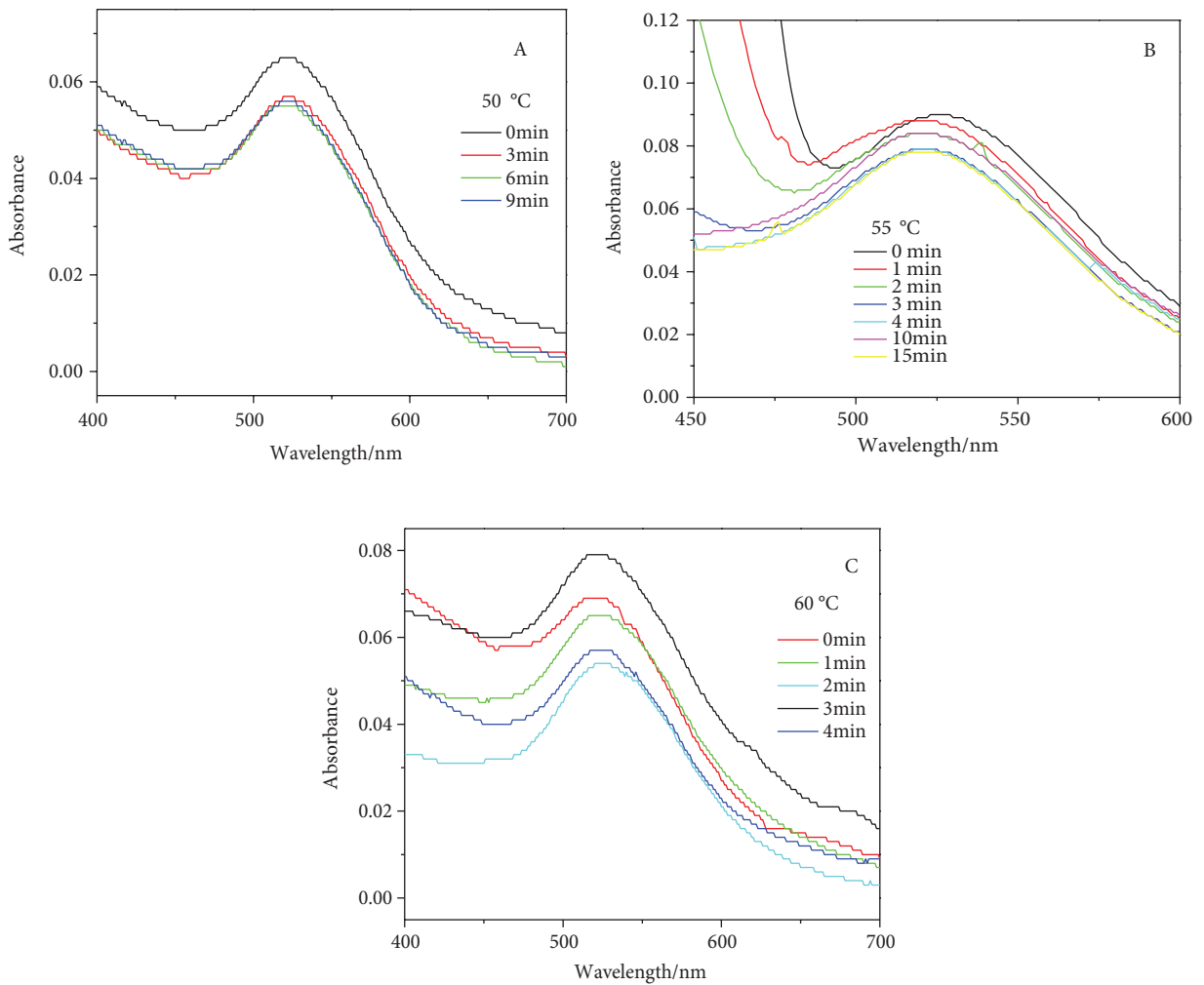


**Figure 3.** GNPs dissolution at higher temperatures 50 °C (A), 55 °C (B), and 60 °C (C) during the course of reduction of 4-NP.

This shows that the extent of the difference in the rate constants gradually decreased as the temperature increased. This may be attributed to the increase in the kinetic energies of the reactants with temperature, which ends in the proximity of both reaction rates. The Arrhenius equation was applied to attain activation energy.

$$\ln k = \ln A - E_a / RT$$

Eq. 2

Here,  $\ln k$  (rate constant) was plotted against  $1/T$  (temperature in K); the frequency factor  $k_0$  was obtained from the intercept, and  $E_a$  was obtained from the slope of the straight line.  $E_a$  was decreased from 30 to 19 kcal/mol for this small increase in catalyst concentration. On the other hand, entropy values were found to increase from 64 to 89 Cal/mol.K. At 50, 55, and 60 °C, the catalyzed reaction was quick enough for the present ratio (1/637000/3076000 catalyst/4NP/BH) to evaluate the kinetic parameters. No induction period  $t_0$  was observed for either of the concentrations of the catalysts, and the reaction began immediately after mixing. With the addition of borohydride, a maximum of 9 nm blue shift was observed after mixing the reactants and the GNPs. This blue shift was not found to be linearly dependent upon BH concentration, and there was a saturation limit after which no further shift was observed. In addition, the SPR of GNPs was not seen to be affected by the 4-NP concentration. This effect and stability were monitored with a UV-Vis spectrophotometer at 30, 35, 40, 45, 50, 55, and 60 °C. It was observed that the concentration of the catalyst plays a vital role in terms of kinetic parameters of the reduction reaction. At slightly higher concentrations of the catalyst, the rate of reduction as well as entropy values increase, while activation energy decreases. However, as the temperature increases, the concentration effect becomes negligible and rate constants for both of the concentrations come into proximity. This could be interpreted as dissolution of the surface gold atoms from GNPs as a result of increase in the kinetic energy of the reactants and solvent molecules and their collisions against the superficial atoms of GNPs, which results in decrease of GNPs size.

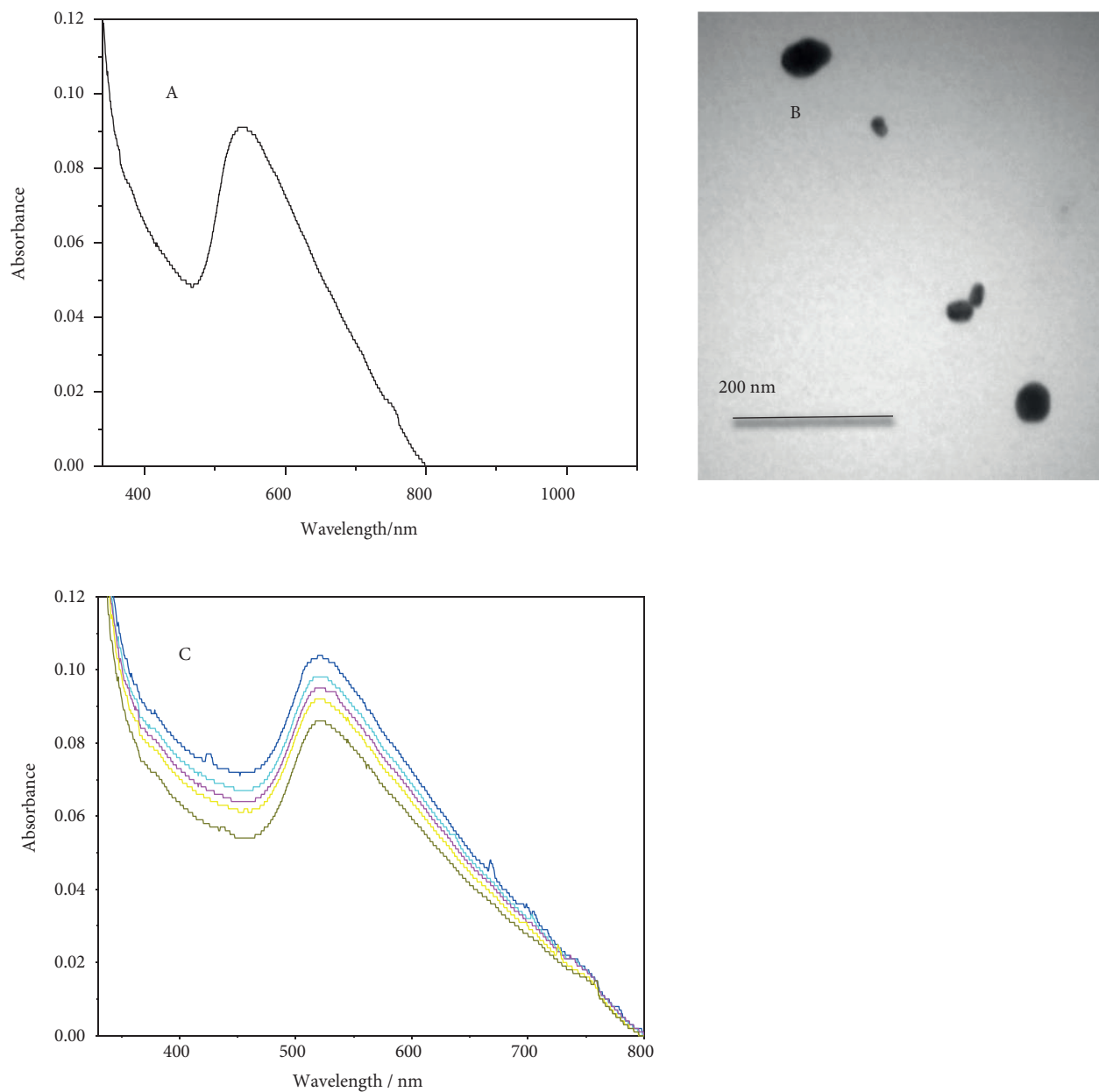


**Figure 4.** UV-visible spectrum (A), TEM image (B) of  $30 \pm 5$  nm gold nanoparticles, and GNPs (30 nm diameter) dissolution at 50 °C during the course of degradation of 4-NP (C).

**Table.** Comparison of kinetic parameters of 4-Nitrophenol reduction reaction at two concentrations of gold nanoparticles.

GNPs conc. (nM)	Rate constant at 35 °C ( $\text{min}^{-1}$ )	Rate constant at 40 °C ( $\text{min}^{-1}$ )	Rate constant at 45 °C ( $\text{min}^{-1}$ )	Activation energy (kcal/mol)	Frequency factor ( $\text{min}^{-1}$ )	Entropy of activation
11.8	$0.019 \pm 1.2 \times 10^{-3}$	$0.04 \pm 9.6 \times 10^{-4}$	$0.09 \pm 2.3 \times 10^{-3}$	$30.24 \pm 1.025$	$3.49 \times 10^{19}$	64.11
15.5	$0.099 \pm 9.9 \times 10^{-4}$	$0.198 \pm 1.1 \times 10^{-2}$	$0.29 \pm 8.3 \times 10^{-3}$	$19.87 \pm 3.417$	$1.03 \times 10^{14}$	89.4

### 3.3. Effect of BH concentration towards stability and reactivity of GNPs

This reduction reaction does not strictly follow pseudofirst-order kinetics, which is why the initial concentrations of 4-nitrophenol, borohydride, and catalyst affect the rate of reaction [37]. The effect of BH concentrations on the stability as

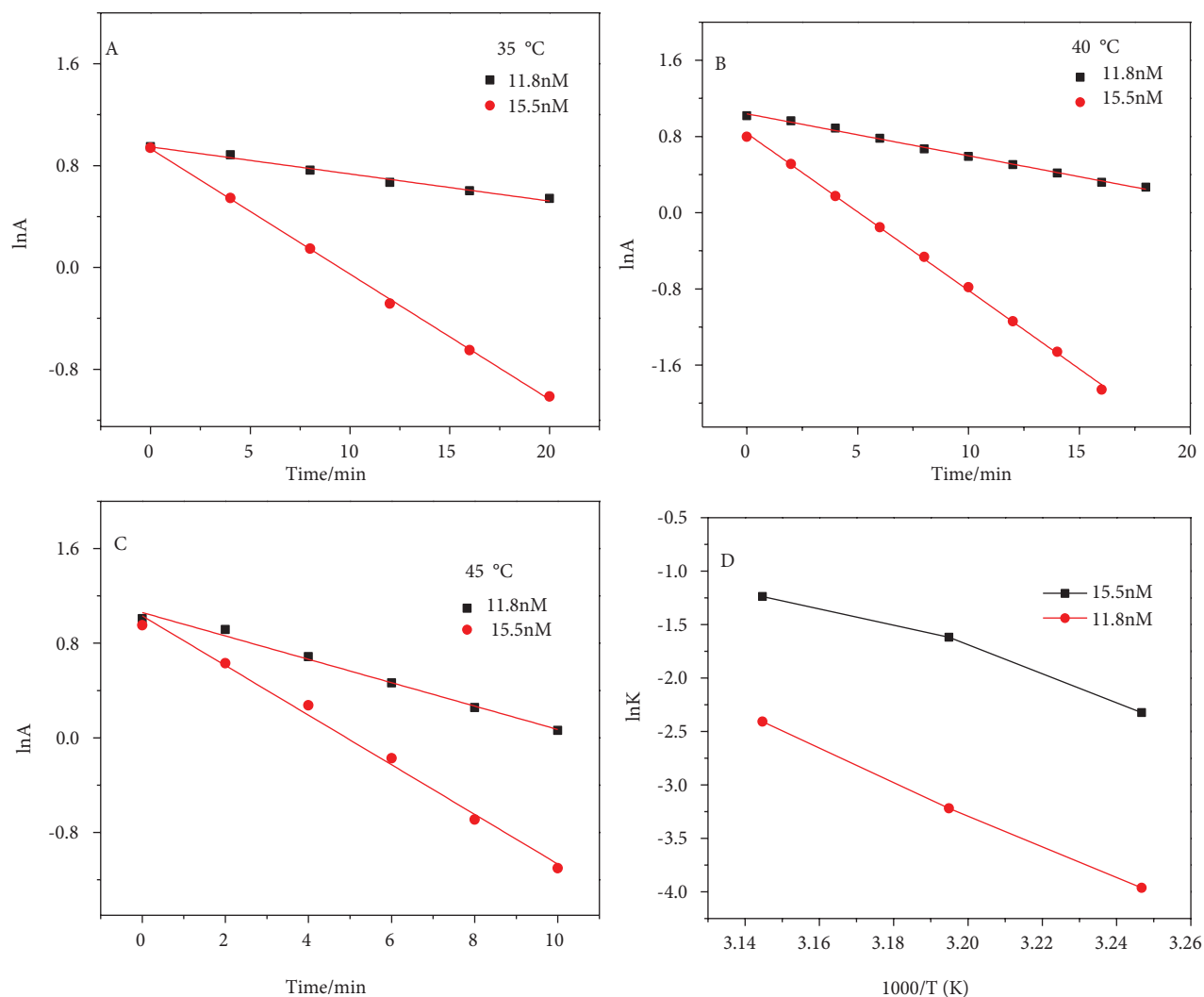


**Figure 5.** Concentration sensitivity of 4-NP reduction process towards GNPs investigated at different temperatures.

well as reactivity of gold nanoparticles during 4-NP reduction was investigated for a range of BH concentrations at room temperature. GNPs were found to be stable (in terms of their consistent optical density) throughout the BH concentration range studied. The dependence of reaction rate on BH concentration is not a linear relationship but a complex one [17,19]. The present studied range shows a linear dependency, although the extent of blue shift was enhanced at the higher concentrations. The higher the hydrid ions surrounding the GNPs, the more displacement of citrate ions will occur [42]; because of this displacement, the SPR shifts toward the lower wavelength region. The extent of the blue shift is because of the change in the refractive index of the surrounding environment of these catalysts, as shown in Figure 6.

The BH adsorbs on the nanoparticle surface and produces  $H_2$  gas and hydrid ion; these lighter species with a refractive index of 1 displace water, which has a refractive index of 1.33. Thus, this particular blue shift is not because of the size, shape, or interparticle distance change for the catalysts, but only because of the refractive index change of their surrounding medium [22,23]. Hence, there was only one abrupt SPR blue shift for these nanocatalysts even after the completion of the whole 4-NP reduction, unlike the gold nanocages, where a time-dependent gradual blue shift was observed because of the inner and outer surfaces of the cavities being available to the reactants [22,23]. The present ratio of GNPs/4NP/BH did not contribute to the aggregation of the GNPs, as reported previously.

BH is known to inject electrons on the exterior surface of gold nanoparticles, which causes the removal of the citrate layer from their surface. If this displacement is effective enough to cause anisotropy of charges on the GNPs' surface, it can lead to the aggregation of the catalyst [15,36]. It has been reported that capping material is usually stripped off during

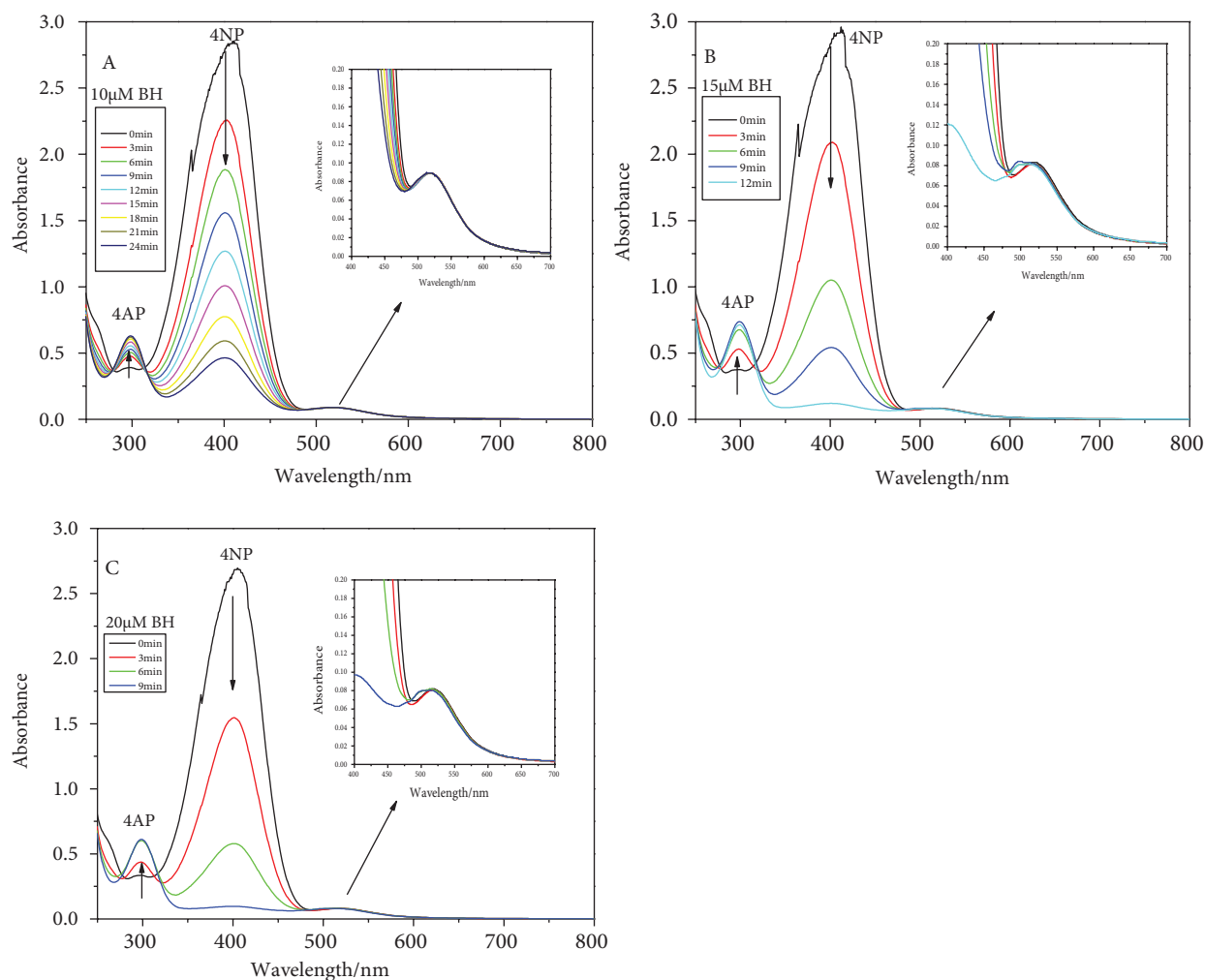


**Figure 6.** SPR stability of GNPs during catalytic reduction of 4-NP at different sodium borohydride concentrations: 10  $\mu\text{M}$  (A), 15  $\mu\text{M}$  (B), and 20  $\mu\text{M}$  (C). A clear blue shift is seen in the cases of 15 and 20  $\mu\text{M}$  concentrations.

the synthesis or catalytic reaction; this may contribute to the nanocatalyst aggregation [15], which was not observed in the present case, with varying concentrations from 10  $\mu\text{M}$  to 20  $\mu\text{M}$ . The Langmuir–Hinshelwood model was applied to interpret this reduction reaction [18,19,21]. According to this model, both reactants must be adsorbed to the exterior of the nanocatalyst to react. This reaction was found to be controlled by kinetics, where the transportation of the reactants through the solution was not the rate-determining step; rather, the formation of 4-AP was the rate-determining step. The adsorbed reactants may react, and the product is desorbed from the exterior of GNPs. In a control experiment, there was no reduction of 4-NP observed in the absence of GNPs or in the presence of trisodium citrate, but gold salt solution was found to degrade 4-NP to some extent. The plausible reason for this effect of gold salt solution was the formation of larger-sized GNPs inside the reaction mixture, which catalyzed this reaction to some extent as depicted in Figure 7.

#### 4. Conclusion

The stability of any catalyst is important during the course of catalytic reaction. We have studied surface plasmon resonance (SPR) stability of colloidal gold nanoparticles during the catalytic reduction of 4-NP (an organic pollutant) at different temperature conditions and BH concentrations. The SPR shift of GNPs or the formation of 4-nitrophenolate ion can be taken as evidence for adsorption of both reactants on the surface of GNPs, proving the Langmuir–Hinshelwood model. The concentration of GNPs varied from 11.8 nM to 15.5 nM at various temperatures. It was found that the rate constant of 15.5 nM GNPs was 5.2 times higher than for the lower concentration at 35  $^{\circ}\text{C}$ ; the difference decreased with increasing

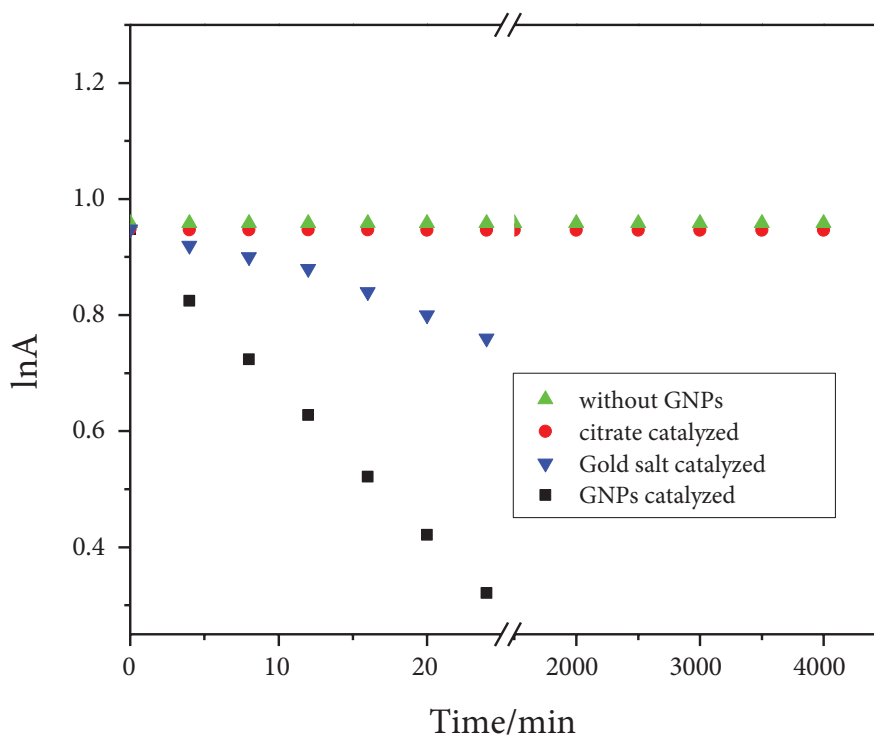


**Figure 7.** Control experiment for 4-NP reduction with borohydride in the presence and absence of GNPs at room temperature.

temperature. This study may find applications in spectrophotometrically designing catalysts for industrial wastewater removal.

### Conflict of interest

The authors declare no conflict of interest regarding the publication of this work.

### References

1. Pradhan N, Pal A, Pal T. Silver nanoparticle catalyzed reduction of aromatic nitro compounds. *Colloids and Surfaces A: Physicochemical and Engineering Aspects* 2002; 196 (2-3): 247-257.
2. Corbett JF. An historical review of the use of dye precursors in the formulation of commercial oxidation hair dyes. *Dyes and Pigments* 1999; 41 (1-2): 127-136.
3. Rode CV, Vaidya MJ, Chaudhari RV. Synthesis of *p*-aminophenol by catalytic hydrogenation of nitrobenzene. *Organic Process Research & Development* 1999; 3 (6): 465-470.
4. Saha S, Pal A, Kundu S, Basu S, Pal T. Photochemical green synthesis of calcium-alginate-stabilized Ag and Au nanoparticles and their catalytic application to 4-nitrophenol reduction. *Langmuir* 2010; 26 (4): 2885-2893.
5. Ghosh SK, Mandal M, Kundu S, Nath S, Pal T. Bimetallic Pt–Ni nanoparticles can catalyze reduction of aromatic nitro compounds by sodium borohydride in aqueous solution. *Applied Catalysis A: General* 2004; 268 (1-2): 61-66.
6. Alhokbany N, Ahama T, Ruksana, Naushad M, Alshehri S. AgNPs embedded N- doped highly porous carbon derived from chitosan based hydrogel as catalysts for the reduction of 4-nitrophenol. *Composites Part B: Engineering* 2019; 173: 106952.
7. Daniel MC, Astruc D. Gold Nanoparticles: Assembly, supramolecular chemistry, quantum-size-related properties, and applications toward biology, catalysis, and nanotechnology. *Chemical Review* 2004; 104 (1): 293-346.
8. Hu M, Chen J, Li ZY, Au L, Hartland GV et al. Gold nanostructures: engineering their plasmonic properties for biomedical applications. *Chemical Society Review* 2006; 35 (11): 1084-1094.

9. Jain PK, Huang X, El-Sayed IH, El-Sayed MA. Noble metals on the nanoscale: Optical and photothermal properties and some applications in imaging, sensing, biology, and medicine. *Accounts of Chemical Research* 2008; 41 (12): 1578.
10. Azetsu A, Koga H, Isogai A, Kitaoka T. Synthesis and catalytic features of hybrid metal nanoparticles supported on cellulose nanofibers. *Catalyst* 2011; 1 (1): 83-96.
11. Thathan P, Lee K, Geckeler KE. Shape-tailoring and catalytic function of anisotropic gold nanostructures. *Nanoscale Research Letters* 2011; 6 (1): 547-559.
12. Kuroda K, Ishida T, Haruta M. Reduction of 4-nitrophenol to 4-aminophenol over Au nanoparticles deposited on PMMA. *Journal of Molecular Catalysis A: Chemical* 2009; 298 (1): 7-11.
13. Narayanan R, Tabor C, El-Sayed MA. Can the observed changes in the size or shape of a colloidal nanocatalyst reveal the nanocatalysis mechanism type: Homogeneous or heterogeneous. *Topics in Catalysis* 2008; 48 (1-4): 60-74.
14. Mahmoud MA, Saira F, El-Sayed MA. Experimental evidence for the nanocage effect in catalysis with hollow nanoparticles. *Nano Letters* 2010; 10 (9): 3764-3769.
15. Mahmoud MA, Synder B, El-Sayed MA. Polystyrene microspheres: inactive supporting material for recycling and recovering colloidal nanocatalysts in solution. *The Journal of Physical Chemistry Letters* 2010; 1 (1): 28-31.
16. Chang YC, Chen DH. Catalytic reduction of 4-nitrophenol by magnetically recoverable Au nanocatalyst. *Journal of hazardous materials* 2009; 165 (1-3): 664-669.
17. Semaginal N, Kiwi-Minsker L. Recent advances in the liquid-phase synthesis of metal nanostructures with controlled shape and size for catalysis. *Catalysis Reviews* 2009; 51 (2): 147-217.
18. Herves P, Pe´rez-Lorenzo M, Liz-Marzan LM, Dzubiel J, Lu Y et al. Catalysis by metallic nanoparticles in aqueous solution: model reactions. *Chemical Society Reviews* 2012; 41 (17): 5577-5587.
19. Wunder S, Polzer F, Lu Y, Mei Y, Ballauff M. Kinetic analysis of catalytic reduction of 4-nitrophenol by metallic nanoparticles immobilized in spherical polyelectrolyte brushes. *The Journal of Physical Chemistry C* 2010; 114 (19): 8814-8820.
20. Carregal RS, Juste JP, Herves P, Liz-Marzan LM, Mulvaney P. Colloidal gold-catalyzed reduction of ferrocyanate (III) by borohydride ions: a model system for redox catalysis. *Langmuir* 2010; 26 (2): 1271-1277.
21. Wunder S, Lu Y, Albrecht M, Ballauff M. Catalytic activity of faceted gold nanoparticles studied by a model reaction: evidence for substrate-induced surface restructuring. *ACS Catalysis* 2011; 1 (8): 908-916.
22. Mahmoud MA, El-Sayed MA. Time dependence and signs of the shift of the surface plasmon resonance frequency in nanocages elucidate the nanocatalysis mechanism in hollow nanoparticles. *Nano Letters* 2011; 11 (3): 946-953.
23. Mahmoud MA, El-Sayed MA. Gold nanoframes: Very high surface plasmon fields and excellent near-infrared sensors. *Journal of the American Chemical Society* 2010; 132 (36): 12704-12710.
24. Mei Y, Lu Y, Polzer F, Ballauff M. Kinetic analysis of catalytic reduction of 4-nitrophenol by metallic nanoparticles immobilized in spherical polyelectrolyte brushes. *The Journal of Physical Chemistry C* 2007; 19 (5): 1062-1069.
25. Panigrahi S, Basu S, Praharaj S, Pande S, Jana S et al. Synthesis and size-selective catalysis by supported gold nanoparticles: study on heterogeneous and homogeneous catalytic process. *The Journal of Physical Chemistry C* 2007; 111 (12): 4596-4605.
26. Chen X, Zhao D, An Y, Zhang Y, Cheng J et al. Formation and catalytic activity of spherical composites with surfaces coated with gold nanoparticles. *Journal of Colloid and Interface Science* 2008; 322 (2): 414-420.
27. Shin KS, Choi JY, Park CS, Jang HJ, Kim K. Facile synthesis and catalytic application of silver-deposited magnetic nanoparticles. *Catalysis letters* 2009; 133 (1-3): 1-7.
28. Arora S, Kapoor P, Singla ML. Catalytic studies of palladium nanoparticles immobilized on alumina synthesized by a simple physical precipitation method. *Reaction Kinetics, Mechanisms and Catalysis* 2010; 99 (1): 157-165.
29. Manesh KM, Gopalan AI, Lee KP, Komathi S. Silver nanoparticles distributed into polyaniline bridged silica network: a functional nanocatalyst having synergistic influence for catalysis. *Catalysis Communications* 2010; 11 (10): 913-918.
30. Zeng J, Zhang Q, Chen J, Xia Y. A comparison study of the catalytic properties of Au-based nanocages, nanoboxes, and nanoparticles. *Nano Letters* 2010; 10 (1): 30-35.
31. Sahiner N, Ozay H, Ozay O, Aktas N. New catalytic route: hydrogels as templates and reactors for in situ Ni nanoparticle synthesis and usage in the reduction of 2- and 4-nitrophenols. *Applied Catalysis A: General* 2010; 385 (1-3): 201-207.
32. Lu Y, Mei Y, Walker R, Ballauff M, Drechsler M. Nano-tree type spherical polymer brush particles as templates for metallic nanoparticles. *Polymer* 2006; 47 (14): 4985-4995.

33. Bhandari R, Knecht MR. Effects of the material structure on the catalytic activity of peptide-templated Pd nanomaterials. *ACS Catalysis* 2011; 1 (2): 89-98.
34. Jiang HL, Akita T, Ishida T, Haruta M, Xu Q. Synergistic catalysis of Au@ Ag core-shell nanoparticles stabilized on metal-organic framework. *Journal of the American Chemical Society* 2011; 133 (5): 1304-1306.
35. Dhiman P, Naushad M, Bato0 KM, Kumar A, Sharma G et al. Nano Fe<sub>x</sub>Zn<sub>1-x</sub>O as a tuneable and efficient photocatalyst for solar powered degradation of bisphenol A from aqueous environment. *Journal of Cleaner Production* 2017; 165: 1542-1556.
36. Kumar A, Sharma G, Al-Muhtaseb AH, Naushad M, Ghfar AA et al. Biochar-templated g-C<sub>3</sub>N<sub>4</sub>/Bi<sub>2</sub>O<sub>2</sub>CO<sub>3</sub>/CoFe<sub>2</sub>O<sub>4</sub> nano-assembly for visible and solar assisted photo-degradation of paraquat, nitrophenol reduction and CO<sub>2</sub> conversion. *Chemical Engineering Journal* 2018; 339: 393-410.
37. Ayad AI, Luart D, Dris AO, Guénin E. kinetic analysis of 4-nitrophenol reduction by “water-soluble” palladium nanoparticles. *Nanomaterials* 2020; 10: 1169.
38. Yukui F, Piao X, Danlian H, Guangming Z, Cui L et al. Au nanoparticles decorated on activated coke via a facile preparation for efficient catalytic reduction of nitrophenols and azo dyes. *Applied Surface Science* 2019; 473: 578-588,
39. Kumar PS, Ramakrishnan K, Kirupha SD, Sivanesan S. Thermodynamic, kinetic, and equilibrium studies on phenol removal by use of cashew nut shell. *Canadian Journal of Chemical Engineering* 2011; 89 (2): 284-291.
40. Frens G. Controlled nucleation for the regulation of the particle size in monodisperse gold suspensions. *Nature (London) Physical Science* 1973; 241 (105): 20-22.
41. Liu X, Atwater M, Wang JH, Huo Q. Extinction coefficient of gold nanoparticles with different sizes and different capping ligands. *Colloids and Surfaces B: Biointerfaces* 2007; 58 (1): 3-7.
42. Zhang Z, Wu Y. Investigation of the NaBH<sub>4</sub>-induced aggregation of Au nanoparticles. *Langmuir* 2010; 26 (12): 9214-9223.